

A MODULAR APPROACH TO DETECTION AND IDENTIFICATION OF DEFECTS IN ROUGH LUMBER

Sang-Mook Lee¹, A. Lynn Abbott¹, and Daniel L. Schmoltdt²

¹Bradley Department of Electrical and Computer Engineering, Virginia Tech, Blacksburg, VA, 24061, USA

²USDA Forest Service, Biological Systems Engineering Department, University of Wisconsin, Madison, WI, 53706-1561, USA

Abstract. This paper describes a prototype scanning system that can automatically identify several important defects on rough hardwood lumber. The scanning system utilizes 3 laser sources and an embedded-processor camera to capture and analyze profile and gray-scale images. The modular approach combines the detection of wane (the curved sides of a board, possibly containing residual bark) with classification of defects. For identifying clear (unblemished) wood, a multilayer perceptron network is used; and for other defects, statistically trained radial-basis-function networks are implemented, followed by a competitive decision scheme. The system is among the first to scan and evaluate lumber in its rough (unplaned) state.

INTRODUCTION

Rough lumber is the principal product resulting from initial log breakdown in a sawmill. These boards often contain residual bark (wane) and other undesirable characteristics (defects) that tend to lower the market value. Saw operators at downstream cutting stations, known as edgers and trimmers, remove portions of each board to reduce wane and to remove some of the defects. Ideally, the selection of these sawing positions should be carefully chosen in order to optimize sale value, which depends on a trade-off of yield (quantity) and grade (quality). Unfortunately, the selection of cutting positions requires complex decisions that are difficult even for trained operators.

A board's grade depends directly on the number and distribution of defects in the wood. Because of this, several efforts have been conducted during the past two decades to develop systems that can automatically detect defects in wooden boards (e.g., [1, 2, 3]). These studies typically involve feature extraction and defect classification based on visual texture properties. In these approaches, image features are extracted and then fed into classifier to distinguish defects from clear wood. In [2], a hierarchical approach to classification is used to improve the resolution of the defect detection and to reduce the computation time.

This paper describes a new classification system that is modular in nature and resembles a decision-tree approach. The system uses both profile (thickness) information and tracheid images obtained from a laboratory scanning system. Three lasers and an embedded-processor camera [4] are used for image acquisition. The profile image is used to remove

background and to detect wane and voids in the wood. Then a modular artificial neural network (MANN), consisting of a multilayer perceptron network (MLPN) and a radial basis function network (RBFN), identifies clear (unblemished) wood and several defect types (voids, knots, and decay).

The next two sections of this paper briefly describe data acquisition and the modular classification approach. Wane detection is described in the following section. The next section describes the MANN approach to classification, and discusses our novel procedure for selecting the number of radial basis functions and optimizing their parameters. Finally, the results of classification experiments are presented, along with a comparison of performance with three different network topologies.

DATA ACQUISITION

Unlike systems using only intensity images or only profile images, our system combines information from both. As shown in Figure 1, profile images are obtained using a sheet-of-light laser source, a video camera, and triangulation. We use the MAPP 2200 camera system [4, 5] to acquire profile images simultaneously with intensity images that exploit the amount of scattering of incident light around the point of influence called "tracheid effect" [6, 7]. This takes advantage of the differential reflectance of laser light in response to grain angle and different densities in the board.

MODULAR DECISION-TREE APPROACH

Figure 2 presents an overview of the modular classification system. Profile images are first analyzed to identify the background and to detect wane and void regions. Simple adaptive thresholding [8] of the profile image effectively removes the background. Wane is then identified within the remaining wood using a novel approach based on surface shape characteristics [9]. Then voids (holes and splits) are determined by simply thresholding the remaining portion of the profile image.

At this point, the procedure has identified the main surface region of the board that must be examined to determine the presence of other defects. Within this portion of the tracheid image, the MANN assigns tentative labels to each pixel. For identifying clear (unblemished) wood, a MLPN is used; and for other defects (knots and decay), a statistically trained RBFN is implemented. A competitive decision scheme resolves the output of the two networks. In order to speed up the process, the MANN examines only "suspicious" regions, which are dark areas as compared to the clear wood. Post-processing, which is still in the preliminary stages, will perform a shape analysis of the regions classified as knots.

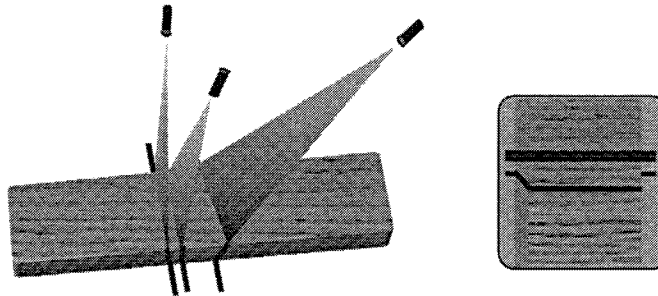


FIGURE 1. Laser arrangement and view from camera. The camera is positioned between the two lasers at the left, so that it looks vertically downward at the board.

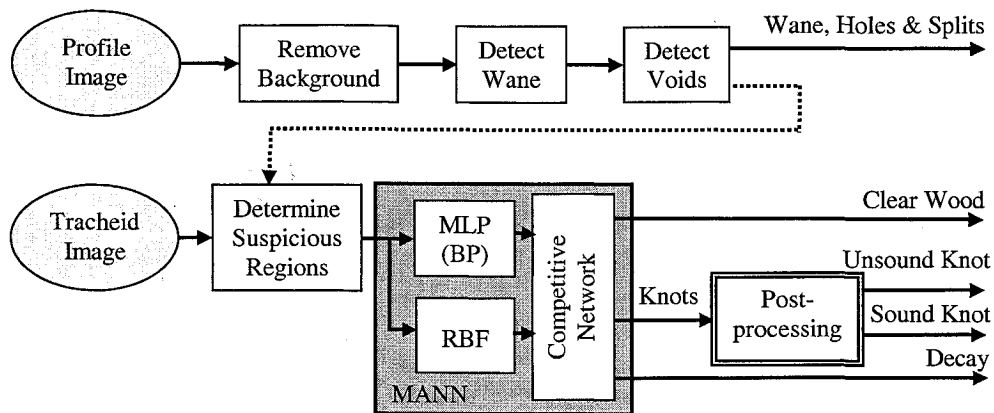


FIGURE 2. Classification block diagram. Two registered images are provided as input. The profile image is first analyzed for shape-based characteristics. The tracheid image is then assessed using a modular artificial neural network to determine the locations of clear wood, knots, and decay.

WANE DETECTION

Wane detection, at first glance, seems to be a simple problem that requires only the selection of a threshold thickness for each board. However, for several reasons including additional bark and debris that is present on rough boards, simple thresholding is not adequate for determining wane regions in a profile image. Therefore, we developed a method for wane detection that depends on surface properties such as orientation and curvature. As described in [9], the system finds local quadratic fits to profile data, and uses this to compute curvature and surface-normal direction. This information is used during a columnwise search for the wane boundary. Related analyses can be found in [10, 11].

MODULAR ARTIFICIAL NEURAL NETWORKS

Introduction

In [12], Jacobs et al. described several advantages that a modular network possesses over a single neural network in terms of learning speed, representation capability, and the ability to deal with hardware constraints. Therefore, if the input space is complex or has a mixture of features from different classes, a modular network is often able to learn faster than a single network because each module responds only one class. In our classification problem, experimental results show that the traditional MLPN often results in unsatisfactory classification performance. On the other hand, the use of a single RBFN to classify all defects of interest along with clear wood requires an exorbitant number of RBFN nodes in the hidden layer.

Because of these concerns, we decided to subdivide the classification problem so that one network distinguishes clear wood from defects, and a second network considers defects only. We selected a small MLPN, using only a small number of nodes in the hidden layer, for the former task. Because of the complexity of the latter problem, we decided to use an RBFN for distinguishing knots from decay. For both network types, careful consideration

must be given to the number of nodes in the hidden layer. We now consider a process for determining the size of the RBF network.

Radial Basis Function Networks

In most RBFN applications, the primary concerns are to determine the kernel function and to select a reasonable number of nodes. A common approach is to select one node per training sample, and then focus on the selection of kernel function parameters [13]. However, but this can result in prohibitive computational costs when the training set is large. On the other hand, if the number of nodes is reduced excessively, then the classification performance can degrade to unacceptable levels.

We have developed a new approach that uses a clustering approach to select the number of nodes, and performs an optimization step to select RBF parameters. We assume radial basis functions of the following form,

$$\phi_{i,c}(\mathbf{x}) = \exp\left(-\alpha_{i,c} \|\mathbf{x} - \mathbf{m}_{i,c}\|^2\right), \quad (1)$$

in which the two parameters $\alpha_{i,c}$ and $\mathbf{m}_{i,c}$ are informally called the “width” and “position” of a node, respectively. This equation represents the c_{th} cluster in class i . During classification, the input feature vector \mathbf{x} is presented to all nodes, and is assigned to the class that is associated with the node that maximizes equation (1).

Clustering

We now consider a clustering algorithm that we have developed to select the number of nodes for each class. It is based on the well-known k -means clustering algorithm [14], which partitions a given sample data set into k clusters such that the normalized sum-of-squared-error criterion, J_e , is minimized:

$$J_e = \sum_{c=1}^k \frac{1}{n_c} \sum_{\mathbf{x} \in \Omega_c} \|\mathbf{x} - \mathbf{m}_c\|^2 \quad (2)$$

$$\mathbf{m}_c = \frac{1}{n_c} \sum_{\mathbf{x} \in \Omega_c} \mathbf{x} \quad (3)$$

The number of clusters, k , is normally assumed to be given in advance. The symbols Ω_c and n_c represent the c_{th} partition of the sample data set and the number of data samples in the partition, respectively. Normally, initial cluster centers \mathbf{m}_c are chosen at random. The algorithm adjusts the centers iteratively using an updating rule. The sample set is regrouped at each iteration by assigning each samples to the nearest cluster center. Limitatons of this algorithms are that prior information of the number of clusters in the sample data set should be known, and a different initial choice of cluster centers can lead to different solutions.

We modified the described alorithm to obtain one that does not need to know the number of clusters in advance. Our algorithm starts with one big cluster (containing all training samples for a given class) and splits the cluster repeatedly. The traditional k -means algorithm selects cluster centers in each case. For $k = 1$, a cluster center is found in this way. To provide the initial centers for $k = 2$, a second cluster center is placed at the location of the data sample that is farthest from the initial cluster center. For each

subsequent case, the cluster with the largest variance is split into two clusters. This *split-and-clustering* procedure continues until the following stopping condition is met:

$$J_e^k - J_e^{k-1} < \delta. \quad (4)$$

We tested this approach using pixel values for knots, taken from trachied images. A total of 550 samples are collected for knots, 200 for clear wood and 200 for decay. Each feature vector consisted of 49 pixel values, taken from a 7x7 neighborhood. The stopping criterion in equation (4) caused the procedure to select 13 clusters to represent this class, as shown in Figure 3. The cluster centers selected by the *k*-means clustering were subsequently used as initial estimates of the node positions, $\mathbf{m}_{i,c}$. To obtain the node width parameters, $\alpha_{i,c}$, we used the largest eigenvalue of the covariance matrix of each cluster.

Optimizing RBF parameters

The *split-and-clustering* algorithm, as described above, provides initial estimates of node sizes and positions for the RBFN. However, because the clustering algorithm deals with each class separately, the initial parameters may need to be adjusted to account for other classes, especially near class boundaries. This adjustment can be obtained through another optimization process that maximizes the following criterion:

$$E = \sum_{i=1}^{\text{number of classes}} \sum_{c=1}^{k_i} \sum_{\mathbf{x} \in \Omega_{i,c}} \phi_{i,c}(\mathbf{x}) \quad (5)$$

We do not change the cluster centers at this stage, but instead allow refinements only in the width parameters, $\alpha_{i,c}$, for each node. In order to obtain optimal values for this, the training data are fed into the initial RBFN, and whenever mis-classification occurs, width parameters for two nodes are updated. For example, assume that data \mathbf{x}_k in class *i* is incorrectly classified as belonging to class *j*, and assume that $\phi_{i,c1}(\mathbf{x}_k)$ and $\phi_{j,c2}(\mathbf{x}_k)$ are the functions that have maximum function values in classes *i* and *j*, respectively. Then, the widths of these two functions are modified as follows:

$$\begin{aligned} \alpha_{i,c1}^{new} &= \alpha_{i,c1}^{old} - \eta \nabla_{\alpha_{i,c1}} E = \alpha_{i,c1}^{old} + \eta \|\mathbf{x} - \mathbf{m}_{i,c1}\|^2 \phi_{i,c1}(\mathbf{x}_k) \\ \alpha_{j,c2}^{new} &= \alpha_{j,c2}^{old} + \eta \nabla_{\alpha_{j,c2}} E = \alpha_{j,c2}^{old} - \eta \|\mathbf{x} - \mathbf{m}_{j,c2}\|^2 \phi_{j,c2}(\mathbf{x}_k) \end{aligned} \quad (6)$$

Every sample data point is tested in this manner and equation (5) is recalculated. This repeats until there is no change in equation (5).

Figure 4 illustrates this refinement by continuing the example described above for all training samples. With this adjustment of the width parameters, the total energy (equation (5)) increases until no further increment is obtained at around 100 iterations.

EXPERIMENTAL RESULTS

The modular decision-tree approach was testing using an oak board, as illustrated in Figure 5. This rough board was scanned soon after being sawed. After detecting wane

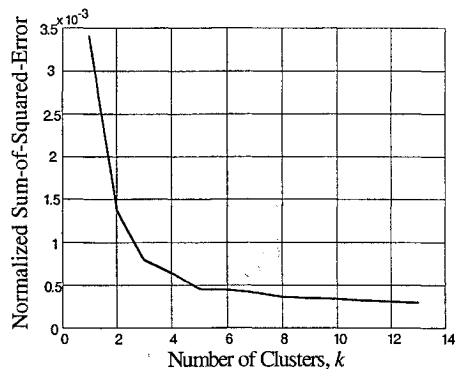


FIGURE 3. Selecting the number of clusters.

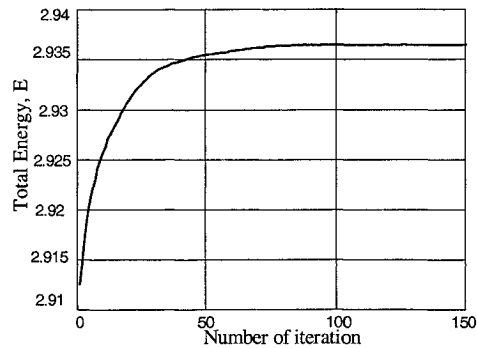


FIGURE 4. Training RBF parameters.

regions by the surface approximation method, the remaining surface of the board was thresholded to determine suspicious regions. This is illustrated in Figure 5(b). Then the MANN examined these regions to classify clear wood, knots and decay (Figure 5(c)). Except for some erroneous results at both ends of the board, the results are quite good. To show the superior performance of our modular approach, we compared it with single networks, and the performance comparison is tabulated in Table 1. We used 10-fold cross-validation to measure the performance in each case. When compared with a single RBFN and with a single MLPN, the MANN exhibited superior performance in our tests.

CONCLUSION

This paper has presented a modular approach for the detection and identification of defects in rough lumber. Profile images, which represent board thickness, are used to detect background, holes, and splits with relative ease. Profile images are also used for detecting wane, which needs special concern because there is a significant amount of noise and debris in this area. For the detection of other defects (knots and decay), we used a modular artificial neural network (MANN). As compared with traditional neural networks, this approach allows for reduced network size and training time. Our MANN combines a multi-layer perceptron network (MLPN), a radial basis function network (RBFN) and a competitive network. The MLPN has the goal of distinguishing clear wood from defects, whereas the RBFN distinguishes knots from decay. The competitive network picks a winner from the two networks' outputs to generate a single classification result for each pixel. The identification of different types of knots is a topic for further study.

To choose an optimum number of radial basis functions for the hidden layer of the RBFN, we have developed a new *split-and-clustering* algorithm. This relies on the repeated use of the well-known *k*-means clustering algorithm. For each class to be identified, the

TABLE 1. Performance comparison of various network topologies.

Fold	1	2	3	4	5	6	7	8	9	10	Avg.	Performance
MANN	87	90	94	91	89	91	95	95	95	92	91.9	96.7%
RBFN	82	84	87	89	85	89	91	92	90	92	88.1	92.7%
MLPN	81	82	88	87	86	85	90	91	87	89	86.6	91.2%

split-and-clustering procedure continues until the addition of new class centers (and equivalently, new nodes in the RBFN) yields negligible improvement in representing all points in the training set for the given class. The resulting initial node parameters are then refined by considering all classes simultaneously.

The automatic detection of wane and defects in lumber is an important aspect of future improvements in sawmill operations. The system described here represents a significant step, and is unusual in that it addresses the scanning of lumber in its rough state.

ACKNOWLEDGEMENTS

This work was partially supported by USDA NRI Competitive Grant #97-36200-5274.

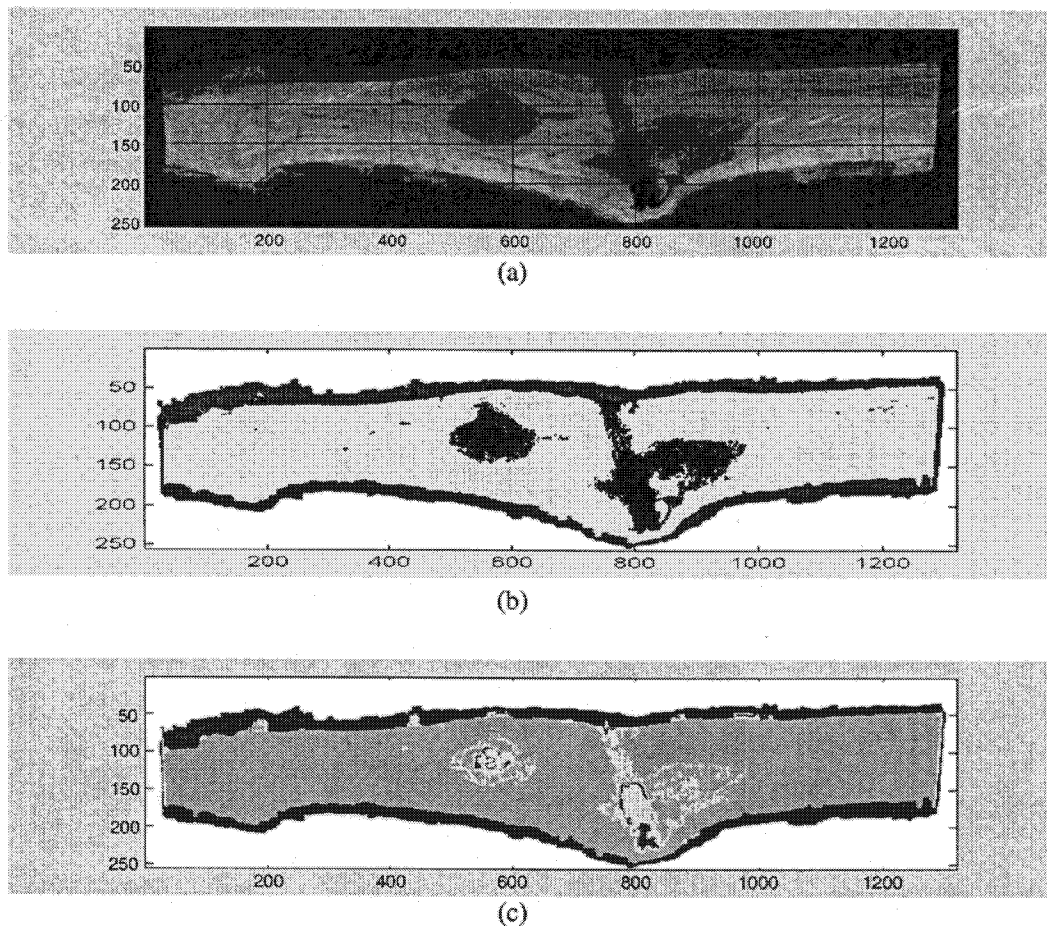


FIGURE 5. Classification result for one board. (a) Trachied image of the board. (b) Intermediate result. Clear wood is indicated by the light gray color; wane is indicated along the upper and lower portions of the board by an intermediate shade of gray; and suspicious points are indicated by black. (c) The final result. Suspicious points have been classified as either clear wood, knots, or decay.

REFERENCES

1. Conners, R.W., McMillin, C.W., Lin, K. and Vasquez-Espinosa, R.E., "Identifying and locating surface defects in wood: Part of an automated lumber processing system", *IEEE Trans. On Pattern Analysis and Machine Intelligence*, vol. **PAMI-5**, no. 6, pp. 573-583 (1983).
2. Kim, C.W. and Koivo, A.J., "Hierarchical Classification of Surface Defects on Dusty Wood Boards", in *Proceedings: 10th International Conference on Pattern Recognition*, vol. 1, 1990, pp. 775 -779.
3. Lee, S.-M., Abbott, A.L., and Schmoldt, D.L., "Using an embedded-processor camera for surface scanning of unplanned hardwood lumber", to appear in *Review of Progress in Quantitative Nondestructive Evaluation*, Thompson, D.O., and Chimenti, D.E. (Eds.), vol. 19, Montreal, Canada, 1999.
4. Forchheimer, R., Ingelhart, P., and Jansson, C., "MAPP2200, a second generation smart optical sensor", in *SPIE Proceedings*, vol. 1659, Arps, R.B. and Pratt, W.K. (Eds.), 1992, pp. 2-11.
5. Åstrand, E., *Automatic inspection of sawn wood*. Ph.D. dissertation, Department of Electrical Engineering, Linköping University, Linköping, Sweden, 1996.
6. Soest, J. F., and Matthews, P. C. "Laser scanning technique for defect detection", in *Proceedings: 1st International Conference on Scanning Technology in Sawmilling*, R. Szymani (Ed.), Oct. 10-11, San Francisco, CA, 1985, pp. XVII-1-4.
7. Matthews, P. C., "Wood, light, and objective scanning", in *Proceedings: 2nd International Conference on Scanning Technology in Sawmilling*, R. Szymani (Ed.), San Francisco, CA, 1987.
8. Otsu, N., "A threshold selection method from gray-level histograms", *IEEE Trans. on Systems, Man, and Cybernetics*, vol. **SMC-9**, no. 1, pp. 62-66 (1979).
9. Lee, S.M., Abbott, A.L. and Schmoldt, D.L., "Wane detection on rough lumber using surface approximation", in *Proceedings: 4th International Conference on Image Processing and Scanning of Wood*, D.E. Kline and A.L. Abbott (Eds.), August, 2000, pp. 115-126.
10. Hoffman, R., and Jain, A.K., "Segmentation and classification of range images", *IEEE Trans. Pattern Analysis and Machine Intelligence*, vol. **PAMI-9(5)**, pp. 608-620 (1987).
11. Besl, J.P., and Jain, R.C., "Segmentation through variable-order surface fitting", *IEEE Trans. Pattern Analysis and Machine Intelligence*, vol. **PAMI-10(2)**, pp. 167-192 (1988).
12. Jacobs, R.A., Jordan, M.I., and Barto, A.G., "Task decomposition through competition in a modular connectionist architecture: The what and where vision tasks", *Cognitive Science* **15**, pp. 219-250 (1991).
13. Bruzzone, L., and Prieto, D.F., "A technique for the selection of kernel-function parameters in RBF neural networks for classification of remote-sensing images", *IEEE Trans. on Geoscience and Remote Sensing*, vol. **37**, No. 2, pp. 1179-1184 (1999).
14. Duda, R.O., and Hart, P.E., *Pattern Classification and Scene Analysis*, Wiley-Interscience, New York, 1973.